Dimensionality crossover and frustrated spin dynamics on a triangular lattice

J. M. Wikberg,[1,*] M. Dahbi,[2] I. Saadoune,[2] T. Gustafsson,[3] K. Edström,[3] and P. Svedlindh[1]
[1]*Department of Engineering Sciences, Uppsala University, P.O. Box 534, SE-75121 Uppsala, Sweden*
[2]*ECME, LP2E2M, FST Marrakech, University Cadi Ayyad, BP 549, Avenue Abdelkrim el Khattabi, Marrakech, Morocco*
[3]*Department of Materials Chemistry, Uppsala University, P.O. Box 538, SE-75121 Uppsala, Sweden*
(Received 13 April 2010; revised manuscript received 6 May 2010; published 7 June 2010)

Investigations of the magnetic behavior of the layered oxide, $LiNi_{0.65}Co_{0.25}Mn_{0.10}O_2$, through ac and time-dependent susceptibility, dc linear and nonlinear susceptibility as well as neutron-diffraction measurements are presented. A ferrimagneticlike spin ordering appears at 119 K with a spontaneous magnetization coexisting with spin frustration in two dimensions (2D). At lower temperature, a cluster-glass transition is found at 17.4 K indicating a transformation to a completely frustrated state in three dimensions (3D). A dimensionality crossover with temperature, from 2D to 3D, in a magnetically frustrated system has been demonstrated. The observed magnetic behavior is believed to originate from a percolating system of spin clusters defined by disordered and frustrated exchange interactions and the findings conform well with predictions of the percolation cluster model.

DOI: 10.1103/PhysRevB.81.224411 PACS number(s): 75.47.Lx, 75.50.Lk, 82.47.Aa

I. INTRODUCTION

Since the first synthesis in 1958 (Ref. 1) and prediction that $LiNiO_2$ may be the first realization of a quantum spin liquid,[2] layered transition-metal (*TM*) oxides of α-$NaFeO_2$ type have been of interest from both theoretical and experimental point of views. The alternating planes of alkali metals (e.g., Li or Na) and triangular-shaped metal-oxide (MO_2) slabs built up of edge-sharing octahedras (MO_6) form a two-dimensional triangular lattice (2DTL). The 2DTL structure offers possibilities to study the interplay between orbital and spin degrees of freedom where much effort has been devoted to probing the magnetic ground state of $LiNiO_2$. A major problem in these studies has been parasitic divalent Ni ions (Ni^{2+}_{3a}) residing in the Li plane ($3a$) which are introduced during the fabrication process and thought to be the reason for the large disparity in the reported magnetic behavior of $LiNiO_2$.[3] Efforts have been made to cancel out the interlayer exchange interactions by minimizing the amount of Ni^{2+}_{3a} or by increasing the interplane distances to obtain a true 2DTL system, e.g., as in $NaNiO_2$ or Ag_2NiO_2.[4,5] In more recent years, a drive for research in $LiTMO_2$ is due to its importance in Li-ion batteries. Since the introduction of the Li-ion battery with $LiCoO_2$ by Sony Corp. in 1990, one has strived to replace Co with other *TM* elements that are more efficient, structurally stable and environmentally more benign. Also, the understanding of the magnetic properties is a crucial component in determining the structural quality and even electrochemical properties in Li-ion battery materials. Recent investigations suggest that the true ground state of $LiNiO_2$ is of a short-range AFM 90° type[6] but the observed magnetic behavior is in most case much more complex. Despite some controversy about the magnetic ground state, lately more consensus about the origin of the magnetism in Ni-containing $LiTMO_2$ has emerged where the divalent Ni ions play a crucial role. First, in the $3a$ plane, Ni^{2+}_{3a} enables magnetic coupling between the MO_2 slab ($3b$) and the $3a$ plane through 180° interlayer superexchange interactions of both ferromagnetic (FM) (e.g., Ni-Mn) and antiferromagnetic (AFM) (Ni-Ni) type. At low temperature, a spin-glass state originating from frustrated superexchange interactions provided by Ni^{2+}_{3a} sitting between the $3b$ planes in $LiNiO_2$ (Ref. 4) occurs for Ni^{2+}_{3a} concentrations as small as 1%.[3] Second, the parasitic Ni^{2+}_{3a} is combined by a similar amount of Ni^{2+}_{3b} creating both divalent and trivalent Ni ions with $S=1$ and 1/2, respectively, in the MO_2 slab. In this study, tetravalent Mn ($S=3/2$) and trivalent Co in its low-spin state ($S=0$) are also present in the MO_2 slab. This adds both FM (Ni-Ni, Mn-Mn) and AFM (Ni-Mn) 90° intralayer exchange interactions to the magnetic structure.[7] Not only are the divalent Ni ions creating competing interactions between planes but also both Ni^{2+}_{3a} and Ni^{2+}_{3b} couple with six other transition-metal ions forming exchange interactions of both the 90° and the 180° type[8] further adding to the importance of controlling the amount of Ni^{2+}_{3a}. The minimization of the electrostatic energy promotes a random distribution of the *TM* ions in both the $3a$ and $3b$ planes and this together with the mixed valency and magnetic dilution, due to the low-spin Co ions, imply that regions of exchange-coupled magnetic ions are formed as a percolating clusterlike pattern in the material.[7,9] While low-temperature spin-glass behavior is well established in $LiNiO_2$, 2DTLs with Mn, e.g., $LiNi_{0.5}Mn_{0.5}O_2$ and Ag_2MnO_2, have shown evidence of long-range spin order[10] and/or an additional frustrated regime at high temperature.[7,11]

In this paper, we present results evidencing both ferrimagneticlike behavior and frustration in $LiNi_{0.65}Co_{0.25}Mn_{0.10}O_2$. By inducing a high concentration of divalent Ni ions in the compound (here 12.4%), a mosaic of magnetic interactions are present in the same material resulting in a highly unusual reentrant behavior with a crossover from percolating ferrimagnetic spin order coexisting with a 2D frustrated state to a 3D cluster-glass state.

II. EXPERIMENTAL

Powder of $LiNi_{0.65}Co_{0.25}Mn_{0.10}O_2$ was synthesized by mixing an aqueous solution containing 1.10 $LiNO_3$ (99%, Aldrich), 0.65 $Ni(NO_3)_2 \cdot 6H_2O$ (99%, Aldrich), 0.25

TABLE I. Structural data from Rietveld refinement of neutron-diffraction data at different temperatures.

	5 K	60 K	120 K	289 K
a_{hex} (Å)	2.8722(3)	2.8720(3)	2.8723(3)	2.8752(3)
c_{hex} (Å)	14.191(5)	14.192(5)	14.197(5)	14.222(5)
c_{hex}/a_{hex}	4.941	4.942	4.943	4.946
V_{hex} (Å^3)	101.385	101.378	101.435	101.819
R_{Bragg}	2.943	2.056	2.976	2.808
R_F	1.877	1.648	1.909	1.873

$Co(NO_3)_2 \cdot 6H_2O$ (>98%, Aldrich), and 0.10 $Mn(NO_3)_2 \cdot 6H_2O$ (99%, Aldrich) with sucrose in a mole ratio of sucrose/nitrate equal to 0.67. The solution was subsequently heated up to 120 °C for 1 h. Finally, the powder was fired up to 1000 °C for 12 h in ambient air (with a heating rate of 1 °C min^{-1}) forming a light downy substance, for further details see Ref. 12. The x-ray diffraction (XRD) patterns were obtained at 298 K on a Siemens D5000 diffractometer with Cu $K\alpha$ radiation. Neutron-diffraction experiments were performed at the Laboratoire Léon Brillouin (CEA-CNRS in Saclay) using the G4.1 diffractometer (wavelength 2.4226 Å) in the temperature range from 5 to 289 K. ac and dc magnetic measurements were performed in a Quantum Design MPMS-XL system. The magnetic susceptibility was measured following zero-field-cooled (ZFC) and field-cooled (FC) protocols with different applied dc magnetic fields (H_{dc}) in the range 0.5–100 Oe. Magnetization (m) versus H_{dc} was measured between $H_{dc} = \pm 10$ kOe at different temperatures (T) in the range 10–140 K. Nonlinear susceptibilities were obtained by measuring the first, second, and third harmonics of the magnetic response to an ac magnetic field (h_{ac}) at zero H_{dc} in a Quantum Design PPMS system. Magnetic relaxation and aging experiments were performed in a specially designed rf-superconducting quantum interference device magnetometer described elsewhere.[13] The sample is cooled in zero field to the measurement temperature (T_m) and kept at a constant T_m for a wait time (t_w) before a small H_{dc} field is applied and the magnetic relaxation $[m_{ZFC}(t)]$ is recorded.

III. RESULTS AND DISCUSSION

A. Structural properties

$LiNi_{0.65}Co_{0.25}Mn_{0.10}O_2$ has a rhombohedral structure (space group $R\bar{3}m$) with hexagonal lattice parameters given in Table I. Through Rietveld refinement, using the FULLPROF program[14] and powder XRD data, 12.4% of Ni^{2+}_{3a} was revealed. Neutron-diffraction measurements confirm the structural data from XRD as well as show that the rhombohedral structure is stable through the whole temperature range with very small changes in c and a axes (see Table I). The neutron results, cf. Fig. 1 for results obtained at 5 and 289 K, also reveal a Li deficiency with the extra Ni^{2+} in the Li plane and an almost full MO_2 layer. This means that the Li layer consists of 0.876 Li^+ and 0.124 Ni^{2+}_{3a} accompanied by an additional amount of Ni^{2+}_{3b} in the MO_2 layer and thus yields the following more accurate formula for the material; $[Li^+_{1-x}Ni^{2+}_x]_{3a}[Ni^{2+}_{0.1+x}Ni^{3+}_{0.55-x}Co^{3+}_{0.25}Mn^{4+}_{0.10}]_{3b}O_2$ with $x=0.124$. With decreasing temperature, a small intensity decrease is seen in the low-angle background but no extra Bragg reflections, neither intensity increase nor any indication of diffuse scattering are detected. Thus, no long-range translational or orientational magnetic order could be confirmed. More on the magnetic implication of the neutron-diffraction results will be discussed later in the text. Both XRD and neutron data indicate a phase pure material free from secondary phases or precipitates.

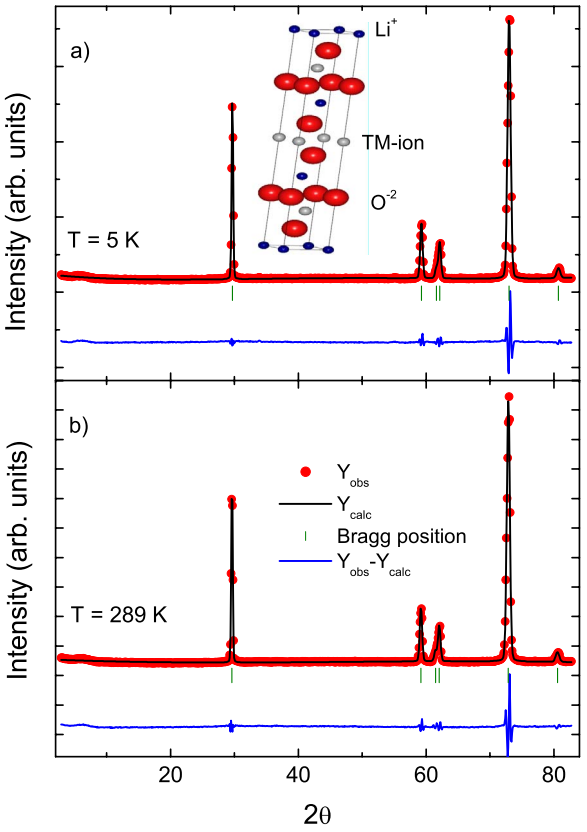

FIG. 1. (Color online) Rietveld refinement on neutron-diffraction data obtained at (a) $T=5$ K and (b) $T=289$ K. The inset of (a) shows the α-$NaFeO_2$-type structure with blue, gray, and red spheres representing the Li, TM, and O ions, respectively.

B. Magnetic properties

The inverse susceptibility $(1/\chi)$, seen in Fig. 2, shows a linear dependence on temperature (T) in the high-T region with a Weiss temperature (θ) of 14 K obtained from a Curie-Weiss fit, $\chi = C/(T-\theta)$, and an effective moment (μ_{eff}) of $2.38\mu_B$ as given by the Curie constant C. This indicates a predominance of FM interactions and the measured μ_{eff} corresponds well with the spin-only effective moment of $2.41\mu_B$ from the Ni and Mn ions. On further cooling, $1/\chi$ displays a ferrimagnetic-type behavior with a transition temperature (T_c) at 119 K. The m versus H_{dc} curves, shown in Fig. 2(c), reveal a magnetization comparably small in magnitude with

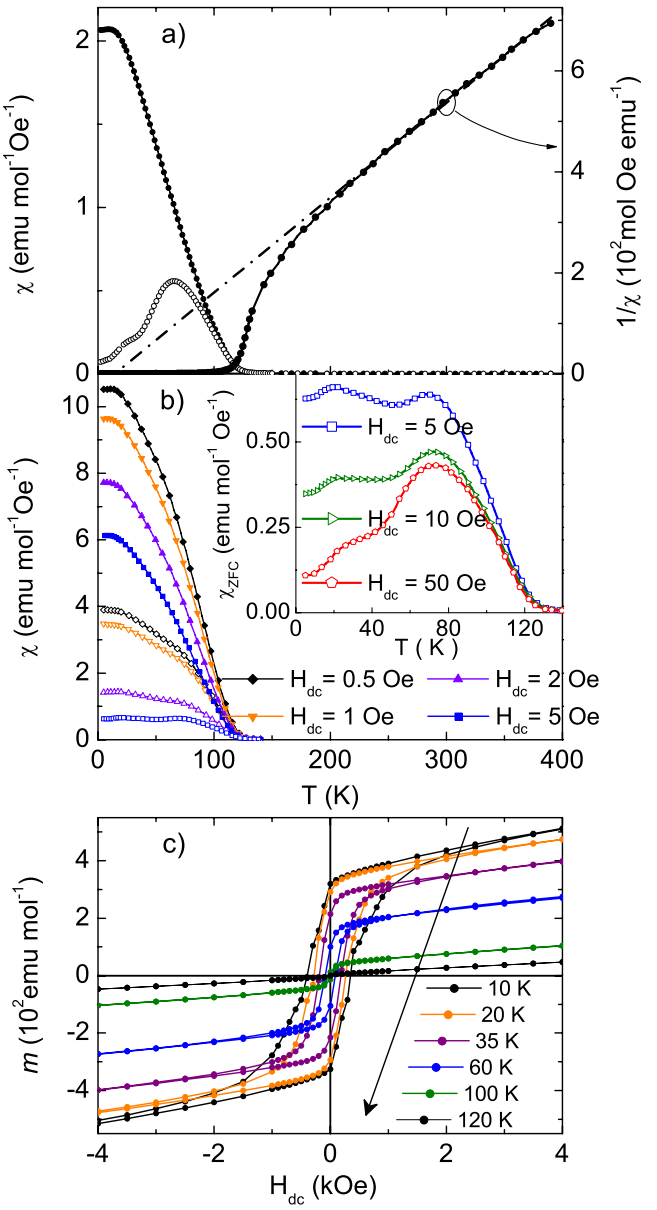

FIG. 2. (Color online) (a) ZFC (open symbols) and FC (filled symbols) susceptibility versus temperature at $H=100$ Oe. The inverse susceptibility $(1/\chi)$, derived from the FC data, versus temperature is also shown. (b) χ_{FC} and χ_{ZFC} versus temperature (open and filled symbols, respectively) under different applied fields ($H_{dc}=0.5$, 1, 2, and 5 Oe). The inset of (b) shows χ_{ZFC} for $H_{dc}=5$, 10, and 50 Oe. (c) m versus H_{dc} at 10, 20, 35, 60, 100, and 120 K between ± 10 kOe with the coercivity (H_c) decreasing with increasing temperature; $H_c=397$ Oe, 280 Oe, 190 Oe, 85 Oe, 31 Oe, and 0 Oe, respectively.

no sign of saturation in the measured field interval (± 10 kOe) and a decreasing coercive field (H_c) with increasing temperature. From zero-field-cooled and field-cooled susceptibility measurements, a divergence between the two measurement protocols is seen at a temperature (T_r) very close to T_c. Below T_r, the χ_{ZFC} displays two cusp temperatures (T_{cusp}), at 70 and 20 K while the χ_{FC} continues to increase in magnitude down to 10 K. The field dependence of the temperature-dependent magnetic susceptibility is shown in Fig. 2(b), where it is seen that both χ_{FC} and χ_{ZFC} are suppressed by even small applied dc fields. A striking feature of the χ_{ZFC} is that the field dependence at $T_{cusp}=20$ K is proportionally much stronger as comparing with that at $T_{cusp}=70$ K; the cusplike feature at 20 K is almost completely suppressed by dc fields $H_{dc}\geq 100$ Oe. The close similarity between T_f and T_c suggests that the material is a spin-cluster system.[15] This is further supported by the monotonic increase in m with H_{dc} without reaching magnetic saturation which together with the H_c increase with decreasing temperature indicate randomly distributed clusters[10,16] consisting of exchange-coupled Ni and Mn moments with internal spin frustration. It should be noted that the clusters mentioned here are not aggregates of magnetic ions but rather random percolating entities defined by magnetic exchange interactions.

The frequency (f) dependence of the in-phase $[\chi'(T)]$ and out-of-phase $[\chi''(T)]$ components of the ac susceptibility is shown in Figs. 3(a) and 3(b), respectively. The χ' and χ'' responses show evidence, with respect to the magnetic behavior, of three different temperature regions. The sharp rise at 120 K is attributed to the ferrimagneticlike ordering seen in the dc measurements. This is followed by a broad temperature region ($40<T<100$ K) where the magnitude of χ'' increases with decreasing f in accordance with the behavior of a 2D frustrated spin state.[17] For spin systems with no phase transition at finite temperature ($T_g\rightarrow 0$) as in the case of a 2D spin glass,[18] a noncritical slowing down following a generalized Arrhenius law, $\ln(\tau/\tau_{o2})\propto T_f^{-(1+\psi\nu)}$, where $\tau=1/(2\pi f)$ and T_f is the spin-freezing temperature, would be expected. Identifying the f-dependent T_{cusp} in χ'' and in the temperature range ($40<T<80$ K) as the spin-freezing temperatures, scaling yields a microscopic relaxation time $\tau_{o2}=5.6\times 10^{-13}$ s, only slightly larger than the atomic spin-flip time,[19] and a critical exponent $\psi\nu=0$ suggesting thermally activated behavior.[20] As the temperature is lowered, the f dependence of χ'' becomes converted in the sense that the magnitude increases with increasing frequency typical for a 3D spin glass.[19] Identifying, in this case, the f-dependent freezing temperature from the inflection point on the upturn of the χ'' curve [cf. Fig. 3(b)] and assuming critical slowing down of the spin dynamics according to $\tau/\tau_{o3}=\epsilon^{-z\nu}$, with $\epsilon=(T-T_{cg})/T_{cg}$, a dynamic critical exponent $z\nu=7.6$, a microscopic relaxation time $\tau_{o3}=4.6\times 10^{-7}$ s, and a cluster-glass transition temperature $T_{cg}=17.4$ K are obtained. The result for $z\nu$ compares well with results obtained for 3D spin-glass[19] and reentrant compounds[21] while the result for τ_{o3} is considerably larger than expected for a spin-glass compound and instead more alike the value expected for a cluster-glass system.[22] The field dependence of the ac susceptibility (with $f=170$ Hz) for both different h_{ac} and H_{dc} fields have also been investigated (not shown). The magnitude of χ' and χ'' increases with h_{ac} as well as with H_{dc} below 120 K down to 65 K. At lower temperature, the field dependence decreases with decreasing temperature and at 20 K, the field dependence for both χ' and χ'' is vanishingly small. A similar behavior has previously been observed for a reentrant spin glass.[21]

A generalized expression for the magnetization in presence of a magnetic field is given by

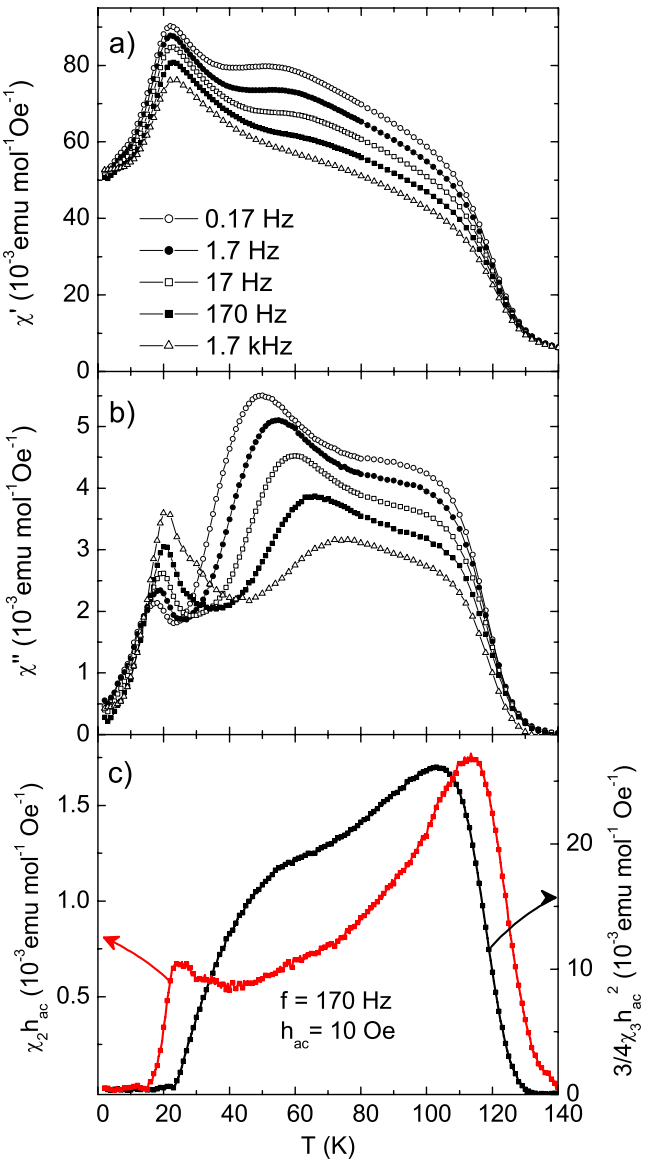

FIG. 3. (Color online) (a) In-phase susceptibility, χ', and (b) out-of-phase susceptibility, χ'', versus temperature at different h_{ac} frequencies. (c) Second $\chi_2 h_{ac}$ (red squares) and third $3/4\chi_3 h_{ac}^2$ (black squares) order nonlinear susceptibilities versus temperature at f=170 Hz, h_{ac}=10 Oe, and H_{dc}=0 Oe.

$$m = m_0 + \chi_1 h + \chi_2 h^2 + \chi_3 h^3 + \cdots, \tag{1}$$

where m_0 is the spontaneous magnetization, χ_1 the linear susceptibility, and χ_2 and χ_3 are the second- and third-order nonlinear susceptibilities, respectively. The χ_2 of the nonlinear susceptibility exhibits two peaks, seen in Fig. 3(c), one at 113 and one at 23 K, with a broad transition in between and an abrupt decrease to zero close to T_{cg}. The χ_3 displays a similar behavior and an appearance coinciding with the behavior of $\chi''(T)$ (the shift downward in temperature of the onset of χ_3 is an illusion caused by the different scales used for the two nonlinear susceptibility components). χ_3 vanishes close to the peak temperature of χ_2, which also coincides with the temperature where χ'' becomes field independent.

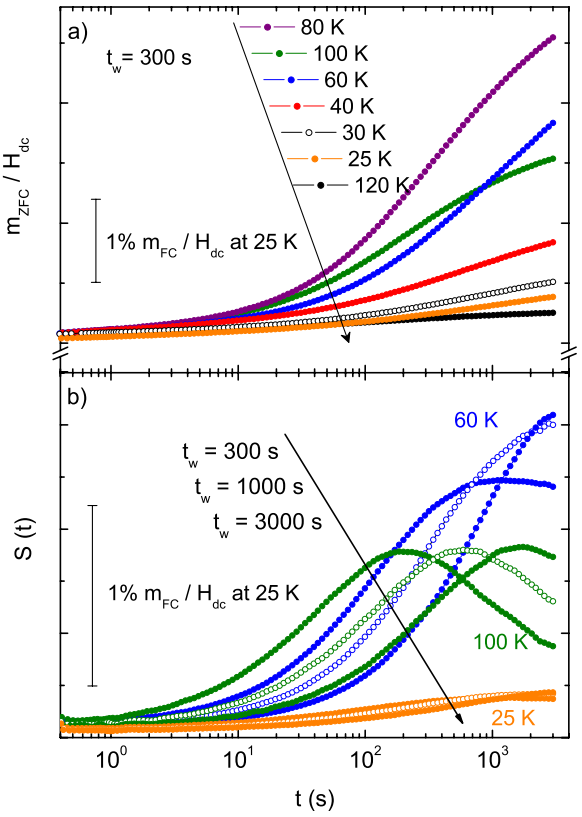

FIG. 4. (Color online) (a) ZFC relaxation of the magnetization (m_{ZFC}/H_{dc}) at H_{dc}=0.40 Oe with t_w=300 s and different T_m=25, 30, 40, 60, 80, 100, and 120 K. (b) Relaxation rate $S(t)$ at 100 K (green), 60 K (blue), and 25 K (orange). H_{dc}=0.40 Oe and t_w =300, 1000, and 3000 s.

The existence of a nonzero second-order nonlinear susceptibility even at zero applied H_{dc} gives clear evidence of a magnetic state with spontaneous magnetization since the magnetization for such a state has no inversion symmetry with respect to the applied field.[23] At the same time, the vanishing of χ_2 close to T_{cg} indicates that there is no spontaneous magnetization below T_{cg}. The χ_3 response appears both for a glassy state[24] and for a ferrimagnetic state; hence, both odd and even nonlinear susceptibility terms are expected.[25]

To further investigate the spin dynamics of the material, magnetic relaxation and aging experiments were performed. The most striking feature of $m_{ZFC}(t)$, shown in Fig. 4(a) for t_w=300 s, is the evolution of $m_{ZFC}(t)$ with T, which is an indication of the development and growth of disordered magnetic clusters with decreasing T. Spin frustration is present at all measured temperatures and aging persists even up to T_c, indicating that clusters of frustrated spins coexist with the ferrimagnetic behavior from the onset of spin ordering. The ZFC relaxation rate $S(t)$ is given by

$$S(t) = \frac{1}{H_{dc}} \frac{\partial m_{ZFC}}{\partial \ln(t)}, \tag{2}$$

where t is the observation time and is plotted in Fig. 4(b) for different t_w and T_m. The behaviors in different temperature

regions are markedly disparate. Starting from high temperatures, in Fig. 4(b) exemplified by the 100 K results, the relaxation rate exhibits maxima (S_{max}) at $t \approx t_w$. However, as the temperature is lowered, S_{max} occurs at $t \gg t_w$, a feature previously observed for 2D spin glasses.[26] Upon further temperature decrease, S_{max} moves back in observation time so that $S_{max}(t \approx t_w)$, a feature which is associated with 3D spin-glass and cluster-glass systems.[22] It is also noteworthy that the ratio defined by the magnitude of the relaxation rate at nonequilibrium and quasiequilibrium conditions, $S_{max}/S(t=1\ \text{s})$, is in comparison to archetypal 3D spin-glass systems very large in the intermediate and high-temperature regions. The large $S_{max}/S(t=1\ \text{s})$ ratio is a feature previously observed in reentrant systems well above T_g.[27] Also, at the lowest temperatures investigated, the $S_{max}/S(t=1\ \text{s})$ ratio is close to values observed for 3D spin-glass systems,[19] which again is an indication of a frustrated system in 3D.

The magnetic-susceptibility measurements reveal a ferrimagneticlike spin ordering at $T_c \approx 119$ K, a feature not supported by the neutron-diffraction results. However, susceptibility measurements yield a bulk average magnetic response that does not give any hint on a possible translational and/or orientational spin order. The combined results imply that the observed ferrimagnetic response descent from a percolating spin system defined by magnetic exchange interactions of varying sign (FM and AFM interactions) and strength. Earlier investigations show that Li-deficient Li$(TM)O_2$ systems exhibit hysteresis as well as ferrimagnetic-type behavior in $1/\chi$ measurements.[7,28] From experimental and theoretical work on $LiNiO_2$, probably the most investigated system, it is well established that Ni^{2+}_{3a} occupies positions in the 3*a* plane at random[3,9] due to minimization of the electrostatic repulsion. The magnetic behavior arises predominantly from AFM Ni-O-Ni 180° superexchange interactions between 3*a* and 3*b* planes.[29] At low temperatures, a spin-glass phase is observed due to frustration created by having AFM superexchange interactions between both 3*a* and 3*b* planes and between neighboring 3*b* planes since the interaction between 3*a* and 3*b* planes will create an effective FM coupling between neighboring 3*b* planes.[3] The introduction of Mn ions in the MO_2 slab is further disturbing the system and investigations on Ag_2MnO_2 (a candidate for an ideal 2DTL system) have shown that the MnO_6 entities have disordered moments in the midtemperature region (<80 K) and short-range AFM order below 30 K.[11] Together with the magnetic dilution due to nonmagnetic Co^{2+}, magnetic disorder is thus introduced[28] which could explain the observed cluster formation and magnetic frustration in 2D as well as in 3D. In addition, recently proposals and evidence of magnetically active $Co^{3+}(S=1/2)$ present in Li-deficient Li(Ni,Co,Mn)O_2 (Refs. 28 and 30) have been presented. This would yield a net increase to the magnetization and further complicate the magnetic state of Li$(TM)O_2$ systems by adding more competing magnetic interactions.

IV. CONCLUSION

In summary, evidences for a reentrant cluster-glass behavior with frustration in both 2D and 3D in $LiNi_{0.65}Co_{0.25}Mn_{0.10}O_2$ have been presented. While the ferrimagnetic quasilong-range ordering is solely due to parasitic Ni^{2+}_{3a}, the 2D cluster-glasslike behavior is due to intralayer exchange interactions of both FM and AFM type in the MO_2 slabs between Ni-Mn, Mn-Mn, and Ni-Ni. Additionally, at low enough temperature, the competing interlayer interactions between 3*a* and 3*b* planes are strong enough to induce a 3D frustrated cluster-glass state without spontaneous magnetization. The disordered and frustrated magnetic behavior stems from the random distribution of *TM* ions in the MO_2 slabs and the inclusion of Ni^{2+} in the Li plane plays a pivotal role since it also implies formation of Ni^{2+} in the 3*b* layers. This in turn leads to the formation of magnetic clusters with exchange interactions of both FM- and AFM-type percolating throughout the system. Neutron-diffraction results show no evidence of translational or orientational spin order and hence support the conclusion that the spin ordering is percolating through the system in a randomized manner.

ACKNOWLEDGMENTS

The authors would like to thank the Swedish Research Council (VR) and the Knut and Alice Wallenberg Foundation (KAW) for financial support. Gilles André is acknowledged for help with the neutron-diffraction measurements.

*magnus.wikberg@angstrom.uu.se

[1] J. B. Goodenough, D. G. Wickham, and W. J. Croft, J. Phys. Chem. Solids **5**, 107 (1958).
[2] K. Hirakawa, H. Kadowaki, and K. Ubukoshi, J. Phys. Soc. Jpn. **54**, 3526 (1985).
[3] E. Chappel, M. D. Nunez-Regueiro, S. de Brion, G. Chouteau, V. Bianchi, D. Caurant, and N. Baffier, Phys. Rev. B **66**, 132412 (2002).
[4] M. J. Lewis, B. D. Gaulin, L. Filion, C. Kallin, A. J. Berlinsky, H. A. Dabkowska, Y. Qiu, and J. R. D. Copley, Phys. Rev. B **72**, 014408 (2005).
[5] J. Sugiyama, Y. Ikedo, K. Mukai, J. H. Brewer, E. J. Ansaldo, G. D. Morris, K. H. Chow, H. Yoshida, and Z. Hiroi, Phys. Rev. B **73**, 224437 (2006).
[6] J. Sugiyama, K. Mukai, Y. Ikedo, P. L. Russo, H. Nozaki, D. Andreica, A. Amato, K. Ariyoshi, and T. Ohzuku, Phys. Rev. B **78**, 144412 (2008).
[7] N. A. Chernova, M. Ma, J. Xiao, M. S. Whittingham, J. Breger, and C. P. Grey, Chem. Mater. **19**, 4682 (2007).
[8] M. D. Núnez-Reguerio, E. Chappel, G. Chouteau, and C. Delmas, Eur. Phys. J. B **16**, 37 (2000).
[9] D. Mertz, Y. Ksari, F. Celestini, J. M. Debierre, A. Stepanov, and C. Delmas, Phys. Rev. B **61**, 1240 (2000).
[10] H. Kobayashi, H. Sakaebe, H. Kageyama, K. Tatsumi, Y. Arachi, and T. Kamiyama, J. Mater. Chem. **13**, 590 (2003).
[11] J. Sugiyama, H. Nozaki, Y. Ikedo, K. Mukai, P. L. Russo, D.

Andreica, A. Amato, H. Yoshida, and Z. Hiroi, Phys. Rev. B **78**, 104427 (2008).
[12] I. Saadoune, M. Dahbi, M. Wikberg, T. Gustafsson, P. Svedlindh, and K. Edström, Solid State Ionics **178**, 1668 (2008).
[13] J. Magnusson, C. Djurberg, P. Granberg, and P. Nordblad, Rev. Sci. Instrum. **68**, 3761 (1997).
[14] J. Rodriguez-Carvajal, Laboratoire Léon Brillouin (CEA-CNRS), http://www-llb.cea.fr/fullweb/powder.html
[15] M. H. Phan, N. A. Frey, H. Srikanth, M. Angst, B. C. Sales, and D. Mandrus, J. Appl. Phys. **105**, 07E308 (2009).
[16] S. Mukherjee, R. Ranganathan, P. S. Anilkumar, and P. A. Joy, Phys. Rev. B **54**, 9267 (1996).
[17] C. Dekker, A. F. M. Arts, H. W. de Wijn, A. J. van Duyneveldt, and J. A. Mydosh, Phys. Rev. B **40**, 11243 (1989).
[18] P. Granberg, P. Nordblad, P. Svedlindh, L. Lundgren, R. Stubi, G. G. Kenning, D. L. Leslie-Pelecky, J. Bass, and J. Cowen, J. Appl. Phys. **67**, 5252 (1990).
[19] P. Svedlindh, P. Granberg, P. Nordblad, L. Lundgren, and H. S. Chen, Phys. Rev. B **35**, 268 (1987).
[20] R. Mathieu and Y. Tokura, J. Phys. Soc. Jpn. **76**, 124706 (2007).
[21] K. Jonason, J. Mattsson, and P. Nordblad, Phys. Rev. B **53**, 6507 (1996).
[22] D. N. H. Nam, K. Jonason, P. Nordblad, N. V. Khiem, and N. X. Phuc, Phys. Rev. B **59**, 4189 (1999).
[23] S. Mukherjee, R. Ranganathan, and S. B. Roy, Phys. Rev. B **50**, 1084 (1994).
[24] M. Suzuki, Prog. Theor. Phys. **58**, 1151 (1977).
[25] A. Chakravarti, R. Ranganathan, and C. Bansal, Solid State Commun. **82**, 591 (1992).
[26] A. G. Schins, E. M. Dons, A. F. M. Arts, H. W. de Wijn, E. Vincent, L. Leylekian, and J. Hammann, Phys. Rev. B **48**, 16524 (1993).
[27] K. Jonason, J. Mattsson, and P. Nordblad, Phys. Rev. Lett. **77**, 2562 (1996).
[28] J. Xiao, N. A. Chernova, and M. S. Whittingham, Chem. Mater. **20**, 7454 (2008).
[29] L. Petit, G. M. Stocks, T. Egami, Z. Szotek, and W. M. Temmerman, Phys. Rev. Lett. **97**, 146405 (2006).
[30] H. M. Hollmark, L. C. Duda, M. Dahbi, I. Saadoune, T. Gustafsson, and K. Edström, J. Electrochem. Soc. (to be published).